Direct numerical simulation of helical vortices

Ivan Delbende*

UPMC, Université Pierre et Marie Curie-Paris 6,
LIMSI-CNRS, UPR3251,
BP133, 91403 Orsay Cedex, France
E-mail: Ivan.Delbende@limsi.fr
*Corresponding author

Maurice Rossi

UPMC, Université Pierre et Marie Curie-Paris 6,
IJLRA-UPMC, UMR7190,
75232 Paris Cedex 05, France
E-mail: Maurice.Rossi@upmc.fr

Benjamin Piton

UPMC, Université Pierre et Marie Curie-Paris 6,
LIMSI-CNRS, UPR3251,
BP133, 91403 Orsay Cedex, France
E-mail: Benjamin.Piton@limsi.fr

Abstract: We herein present a direct numerical simulation method aimed at describing the dynamics of helical vortices such as those developing in the wake of propellers and wind turbine or helicopter rotors. By enforcing a helical symmetry, the 3D incompressible Navier-Stokes equations are reduced to a 2D problem which we solve using a generalised vorticity/streamfunction formulation. In this framework, we simulate the viscous dynamics of one or several helical vortices and describe quasi-steady states as well as long-time (or far-wake) dynamics. In particular, several types of merging in the two helical vortex systems are identified.

Keywords: vortex dynamics; vortex merging; helical vortices; Navier-Stokes equations; numerical simulation.

Reference to this paper should be made as follows: Delbende, I., Rossi, M. and Piton, B. (2012) 'Direct numerical simulation of helical vortices', *Int. J. Engineering Systems Modelling and Simulation*, Vol. 4, Nos. 1/2, pp.94–101.

Biographical notes: Ivan Delbende completed his studies in Physics and Mechanics at the Ecole Normale Supérieure de Lyon (France) and did his PhD at the Ecole Polytechnique in the LadHyX Laboratory under the supervision of Patrick Huerre and Jean-Marc Chomaz. He is now an Assistant Professor at Université Pierre et Marie Curie (UPMC, Paris 6) and works in the fields of open flow instabilities and vortex dynamics in the laboratory LIMSI-CNRS at Orsay.

Maurice Rossi completed his studies in Physics at the Ecole Normale Supérieure de Saint-Cloud (France) and did his PhD at Université Pierre et Marie Curie (UPMC, Paris 6) under the supervision of Gérard Iooss. He is now a Researcher at CNRS, UPMC and works in the fields of instabilities, vortex and lake dynamics in the Laboratory IJLRA in Paris.

Benjamin Piton obtained his Master's degree in Physics from Université Pierre et Marie Curie (UPMC, Paris 6). He is about to defend his PhD thesis (October 2011) in Fluid Dynamics. He is supervised by Ivan Delbende and Maurice Rossi at the Laboratory LIMSI – CNRS at Orsay, and is granted from UPMC.

This paper is a revised and expanded version of a paper entitled 'DNS of helical vortices' presented at the 46th Applied Aerodynamics Symposium of the French Aeronatics and Astronautics Society, Orléans, 28th–29th March 2011.

1 Introduction

Rotating devices such as propellers, wind turbines, helicopter rotors are known to develop a system of helical vortices in their wake. These structures result from the rapid roll-up of the vorticity sheet continuously generated at the trailing edge of the rotating blades. Experiments show that they interact with the mean flow: the radius of helical tip vortices follows the expansion (resp. the contraction) of the fluid tube passing through the turbine (resp. the propeller) and becomes constant within a downstream distance comparable to the diameter of the rotating device. At this distance, the fluid system – apart from turbulent fluctuations – has locally become helically symmetrical, meaning that it is locally invariant through combined axial translation and rotation about the same axis. In most real situations, this property does not hold into the far wake: instabilities often develop and drive the system to a fully three-dimensional turbulent flow. In some cases, a bifurcation may lead to a completely different wake structure, as in the case of the vortex ring state in helicopter flight (Green et al., 2005). In all instances however, it is of great interest to have a reliable description of the reference helical flow at sufficiently high Reynolds number, so that its subsequent evolution can be predicted, for instance, by standard instability theory.

Earlier descriptions of such helical vortex systems made use of the vortex-filament model. On one hand, Hardin (1982) gives an expression for the velocity field induced by a helical vortex filament on the surrounding fluid. This is useful to compute the angular velocity induced by this vortex onto another vortex of the wake (mutual induction). On the other hand, it is also necessary to evaluate the velocity induced by the vortex filament on itself (self-induction). This can be done either by the cutoff theory (Saffman, 1992) whereby the singularity of the filamentary Biot-Savart law is removed (Widnall, 1972; Moore and Saffman, 1972) or by directly removing the singularity on Hardin's solution (Kuibin and Okulov, 1998). Further extensions to helical vortex tubes with finite core size have also been developed (Fukumoto and Okulov, 2005). All these studies are aimed at analytically predict the motion of a helical vortex system with prescribed geometry (helix radius, helix pitch and, when necessary, vorticity distribution within the core).

In the small core limit and in the inviscid framework, such solutions are known to be 'shape-preserving', meaning that they are stationary in a reference frame rotating at the angular velocity predicted for the system. When the core size is finite, the question is raised whether a given vorticity distribution may yield a stationary state or not. In a numerical study, Lucas and Dritschel (2009) recently answered this question for the particular case of inviscid helical vortex patches (uniform vorticity within the core) with prescribed helix radius and vortex core size. Note that the above studies are all strictly restricted to the inviscid framework, a condition for the existence of stationary motion without any forcing.

As mentioned before, wake vortices form through the roll-up of the trailing vorticity sheet, and viscous diffusion eventually leads to continuous distributed vorticity distributions within the vortex cores, such as Gaussian. Moreover, a distribution of axial velocity may also be present, which has always been disregarded in the literature. The complexity of this general problem would lead to use a three-dimensional DNS code. However, the attainable Reynolds numbers are still moderate and long-time dynamics clearly out of reach with nowadays facilities. We present here an original numerical code aimed at describing the viscous dynamics of helical vortex systems, and more generally helically symmetrical flows by direct numerical simulation of the incompressible Navier-Stokes equations. The enforcement of the helical symmetry allows one to reduce the three-dimensional equations to a modified two- dimensional unsteady problem. The code thus takes into account 3D vortex curvature and torsion effects through the helical symmetry, but the resolution is of a 2D type, allowing for larger numbers of grid points and Reynolds numbers.

The Navier-Stokes equations with helical symmetry are presented in Section 2. The numerical formulation is described in Section 3. Viscous quasi-steady states consisting in one or several helical vortices are presented in Section 4. Long-time (or equivalently far-wake) dynamics have also been investigated and different types for the merging of two helical vortices are presented in Section 5. Concluding remarks are given in Section 6.

2 Navier-Stokes equations with helical symmetry

A flow displays *helical symmetry of helix pitch* $2\pi L$ along a given axis when its velocity field is unaffected by an axial translation given by a length parameter Δz followed by a rotation of angle $\Delta\theta = \Delta z \,/\, L$ around the same axis as depicted in Figure 1. The flow characteristics remain invariant along the helical lines $\theta - z \,/\, L = \text{const.}$ $L > 0$ corresponds to a right-handed helix and $L < 0$ to a left-handed helix.

Figure 1 Right-handed helix of reduced pitch L (see online version for colours)

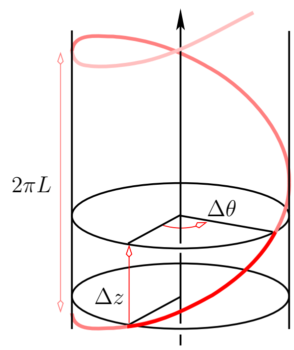

Denoting time by the variable t, an unsteady scalar field $f(t)$ possesses helical symmetry if it depends only, besides time, on the two space variables r and $\varphi \equiv \theta - z \,/\, L$ instead of the three coordinates r, θ and z. For a vector field $u(t)$, helical symmetry means that it can be written as

$$\begin{aligned} u &= u_r(r,\varphi,t)e_r(\theta) \\ &+ u_\varphi(r,\varphi,t)e_\varphi(r,\theta) \\ &+ u_B(r,\varphi,t)e_B(r,\theta) \end{aligned} \tag{1}$$

where the orthogonal Beltrami basis (e_r, e_φ, e_B), presented in Figure 2, is such that

$$\begin{aligned} e_B(r,\theta) &= \alpha(r)\left[e_z + \frac{r}{L}e_\theta(\theta)\right], \\ e_\varphi(r,\theta) &= e_B \times e_r = \alpha(r)\left[e_\theta(\theta) - \frac{r}{L}e_z\right] \end{aligned} \tag{2}$$

with quantity $\alpha(r)$ defined as

$$\alpha(r) = \left(1 + \frac{r^2}{L^2}\right)^{-\frac{1}{2}}, \quad 0 \le \alpha(r) \le 1. \tag{3}$$

Figure 2 Local helical basis (see online version for colours)

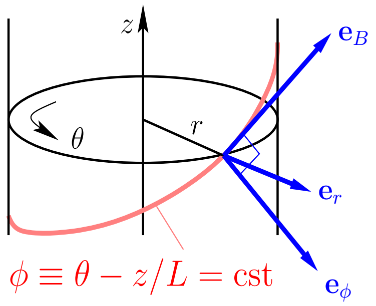

A general incompressible helical flow can be expressed with only two scalar fields as:

$$u = u_B(r,\varphi,t)e_B + \alpha(r)\nabla\psi(r,\varphi,t) \times e_B \tag{4}$$

where $u_B(r, \varphi, t)$ is the velocity component along $e_B(r, \theta)$ and $\psi(r, \varphi, t)$ is a streamfunction. Note that the vorticity field can be expressed as follows:

$$\omega = \omega_B(r,\varphi,t)e_B + \alpha\nabla\left(\frac{u_B(r,\varphi,t)}{\alpha}\right) \times e_B. \tag{5}$$

The vorticity component along e_B is linked to the streamfunction ψ *as well as* to u_B by the following relationship

$$\omega_B = -\mathbb{L}\psi + \frac{2\alpha^2}{L}u_B \tag{6}$$

where the linear operator $\mathbb{L}$ stands for

$$\mathbb{L}(\cdot) = \frac{1}{r\alpha}\frac{\partial}{\partial r}\left(r\alpha^2\frac{\partial}{\partial r}(\cdot)\right) + \frac{1}{r^2\alpha}\frac{\partial^2}{\partial\varphi^2}(\cdot). \tag{7}$$

The total vorticity and velocity fields are thus given by only two scalar fields $\omega_B(r, \varphi, t)$ and $u_B(r, \varphi, t)$. The streamfunction $\psi(r, \varphi, t)$ is slaved to these variables through equation (6).

In order to describe the flow evolution, we hence have to obtain two dynamical equations for quantities $\omega_B(r, \varphi, t)$ and $u_B(r, \varphi, t)$. This formulation is a generalisation of the standard 2D ψ-ω method. Indeed the 3D Navier-Stokes problem for a helical symmetric flow can be reduced to a dynamical equation for $u_B(r, \varphi, t)$ and $\omega_B(r, \varphi, t)$. The first equation reads as

$$\partial_t u_B + NL_u = VT_u \tag{8}$$

where the non-linear and viscous terms are given by

$$\begin{aligned} NL_u &\equiv e_B \cdot [\omega \times u], \\ VT_u &\equiv \nu\left[\mathbb{L}\left(\frac{u_B}{\alpha}\right) - \frac{2\alpha^2}{L}\omega_B\right]. \end{aligned} \tag{9}$$

The dynamical equation for ω_B reads

$$\partial_t \omega_B + NL_\omega = VT_\omega \tag{10}$$

where the non-linear is given by

$$NL_\omega \equiv e_B \cdot \nabla \times [\omega \times u], \tag{11}$$

and the viscous term by

$$\begin{aligned} VT_\omega &\equiv -\nu\, e_B \cdot \nabla \times [\nabla \times \omega] \\ &= \nu\left[\mathbb{L}\left(\frac{\omega_B}{\alpha}\right) - \frac{2\alpha^2}{L}\omega_B + \frac{2\alpha^2}{L}\mathbb{L}\left(\frac{u_B}{\alpha}\right)\right] \end{aligned} \tag{12}$$

More details can be found in Delbende et al. (2011).

3 Numerical formulation

As variable $\varphi = \theta - z / L$ is 2π-periodic, the fields can be expressed as Fourier series along that direction. We hence introduce the 'azimuthal' modes $u_B^{(m)}(r,t)$, $\omega_B^{(m)}(r,t)$ and write equations (8) and (10) for each Fourier mode m (m is a positive integer). For the axisymmetric mode $m = 0$, the dynamical equations are written for the real Fourier modes $u_B^{(0)}(r,t)$ and $u_\varphi^{(0)}(r,t)$, instead of $\omega_B^{(0)}(r,t)$. From quantities $u_B^{(m)}(r,t)$, $\omega_B^{(m)}(r,t)$ for $m \ne 0$, one obtains the values $\psi^{(m)}(r, t)$ for $m \ne 0$ using equation (6) written for mode m:

$$\mathbb{L}^{(m)}\psi^{(m)} = -\omega_B^{(m)} + \frac{2\alpha^2}{L}u_B^{(m)} \tag{13}$$

where the operator $\mathbb{L}^{(m)}$ is given by

$$\mathbb{L}^{(m)}(\cdot) = \frac{1}{r\alpha}\frac{\partial}{\partial r}\left(r\alpha^2 \frac{\partial}{\partial r}(\cdot)\right) - \frac{m^2}{r^2\alpha}(\cdot), \tag{14}$$

together with the boundary conditions for $\psi^{(m)}(r, t)$. The time evolution of mode $u_B^{(m)}(r,t)$ is governed by

$$\partial_t u_B^{(m)} + NL_u^{(m)} = VT_u^{(m)}. \tag{15}$$

As the viscous term VT_u is a linear term, one directly obtains

$$VT_u^{(m)} = \nu\left[\mathbb{L}^{(m)}\left(\frac{u_B^{(m)}}{\alpha}\right) - \frac{2\alpha^2}{L}\omega_B^{(m)}\right]. \tag{16}$$

There is no such simple expression for non-linear terms: NL_u has to be first evaluated in the physical space and is then Fourier-transformed to yield $NL_u^{(m)}$. The time evolution for modes $\omega_B^{(m)}(r,t)$ with $m \neq 0$ and mode $u_\varphi^{(0)}(r,t)$ is treated in a similar way. The code has been adapted from a pure 2D code written by Daube (1992). The time advance of any of these modes is performed using second order backward discretisation of the temporal derivative. Non-linear terms appear explicitly through second order Adams-Bashforth extrapolation whereas the viscous term has been made implicit.

Boundary conditions should be also imposed for $\omega_B^{(m)}$ with $m \neq 0$, $u_B^{(m)}$ and $u_\varphi^{(0)}$. In addition to regularity conditions at $r = 0$, one should impose conditions at the outer boundary taken to be at $r = R_{ext}$:

$$\begin{aligned} &\omega_B^{(m)}(R_{\text{ext}}) = 0,\ u_B^{(m)}(R_{\text{ext}}) = 0 \ \text{ for } m \neq 0, \\ &u_B^{(0)}(R_{\text{ext}}) = \alpha(R_{\text{ext}})\left(U_z^\infty + \frac{\Gamma}{2\pi\Gamma}\right). \end{aligned} \tag{17}$$

A boundary condition for $u_\varphi^{(0)}$ is also imposed at the outer boundary. These conditions are described in a much more detailed way in Delbende et al. (2011).

For spatial discretisation, two series of N_r grid points are defined in the radial direction:

$$\left| \begin{aligned} &r_i = (i-1)\delta r \\ &r_i^+ = r_{i+\frac{1}{2}} = r_i + \delta r / 2 \end{aligned} \right. \quad (i = 1, \cdots, N_r),$$

where $\delta r = R_{ext} / (N_r - 1)$ and only one set of N_θ grid

$$\varphi_j = j\delta\varphi \ \ (j = 0, \cdots, N_\theta - 1), \ \ \varphi_{N_\theta} = \varphi_0 = 0,$$

where $\delta\varphi = 2\pi / N_\theta$. In physical space, quantities $u_B(r, \varphi, t)$, $\omega_B(r, \varphi, t)$, $\psi(r, \varphi, t)$ radial components $u_r(r, \varphi, t)$ and $\omega_r(r, \varphi, t)$ are defined at points (i, j) (which stands thereafter for (r_i, φ_j). Azimuthal components $u_\varphi(r, \varphi, t)$ and $\omega_\varphi(r, \varphi, t)$ live at points $(i + \frac{1}{2}, j)$.

Non-linear terms such as $NL_u^{(m)}$ are needed at points r_i, so that we have to compute the non-linear terms $NL_u = (\omega \times u)_B = \omega_r\, u_\varphi - \omega_\varphi\, u_r$ in physical space at points (i, j). To summarise, one needs to evaluate various quantities at different grid points: $\omega_r\, u_\varphi$, $\omega_\varphi\, u_r$ at points (i, j), $\omega_B\, u_r$ at points $(i + \frac{1}{2}, j)$, $-\omega_B\, u_\varphi$ at points (i, j) and u_B^2 at points (i, j).

The resolution of the dynamical equations requires the radial discretisation of operators $\mathbb{L}^{(m)}$, $VT_u^{(m)}$, $VT_\omega^{(m)}$ at each radial location r_i with $2 \leq i \leq N_r - 1$. This is performed with a second order centred scheme: according to the dynamical equation considered, the resulting system has a tridiagonal, pentadiagonal or hexadiagonal structure, and is solved using a band *LU* factorisation of the LAPACK library. As each mode m is treated independently, parallel computing with shared memory can be most conveniently implemented.

4 Quasi-steady helical vortices

Here we simulate the evolution of a single helical vortex with small core size at a low pitch value. The initial profile is given by

$$\omega_B = \frac{\Gamma_0}{\pi a_0^2}\exp\left[-(r - r_0)^2 / a_0^2\right], \tag{18}$$

and

$$\frac{u_B}{\alpha} = \frac{\Gamma_0}{2\pi L}. \tag{19}$$

In the above formulas and hereafter, quantities are dimensionless, scaled with the helix radius R as space scale, quantity R^2 / Γ as time scale, where Γ is a typical vortex circulation. Here, $\Gamma_0 = \pi$, $r_0 = (1, 0)$, $a_0 = 0.1$ and we set the reduced pitch to $L = 0.5$. The Reynolds number is $Re_0 = \Gamma_0 / \nu = 1{,}000$. The numerical simulation is performed with a domain of radial extent $R_{ext} = 2$ meshed by $N_r \times N_\theta$ grid points, where $N_r = 512$ and $N_\theta = 384$.

The temporal evolution of the helical vorticity component ω_B is shown on Figure 3. At short times, small helical filaments are rapidly formed ($t = 0.08$, 0.012) and destroyed ($t = 0.2$, 0.4). Indeed, the vortex tube as a whole engenders a local strain. As the initial condition is not an inviscid equilibrium state, strain is not counterbalanced by advection. Similarly to the purely 2D vortex case subjected to an external strain, the vortex reaches equilibrium by emitting filaments at its boundary. Thereafter the vortex adopts a shape that remains nearly constant. For $t > 0.4$, it evolves on a slow time scale imposed by viscous diffusion and proportional to the Reynolds number. The helical vortex has thus reached a quasi-steady state when considered in a reference frame rotating with it at frequency ω.

Figure 3 Convergence of a single helical vortex with $L = 0.5$ towards a quasi-steady state: temporal evolution of the helical vorticity component ω_B at $Re_0 = 1{,}000$, viewed in a plane perpendicular to the helix axis (see online version for colours)

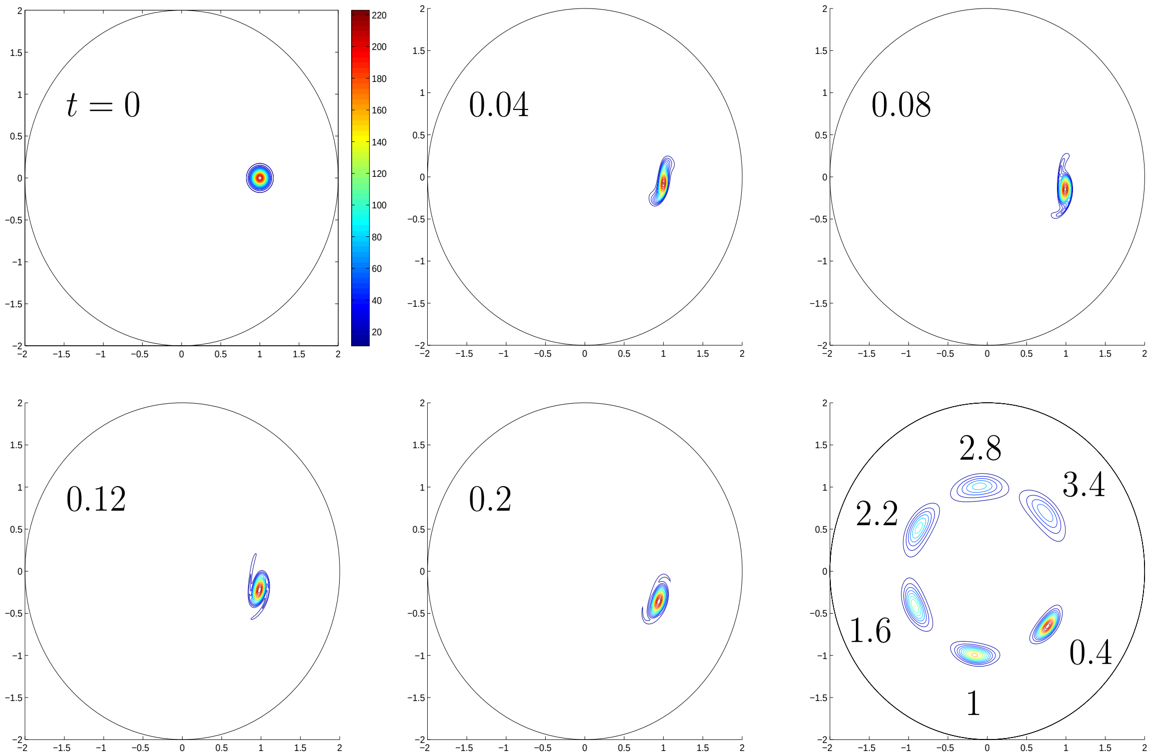

Note: The initial vortex is such that $\Gamma_0 = \pi$, $r_0 = \| r_0 \| = 1$, $a_0 = 0.1$.

Figure 4 Angular velocity $\omega(t)$ of the helical vortex of Figure 3 (see online version for colours)

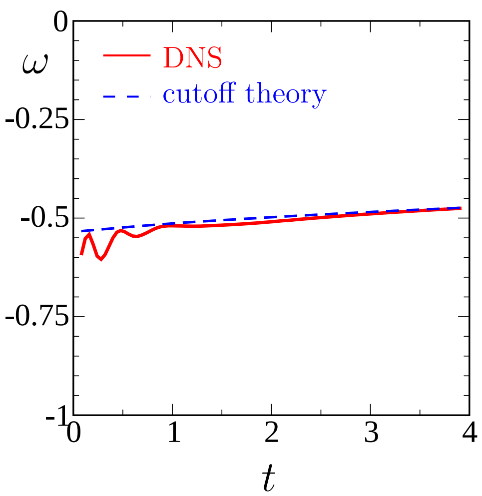

Note: Comparison between DNS and semi-analytical cutoff theory.

Figure 5 Quasi-steady state for two vortices represented in 3D (see online version for colours)

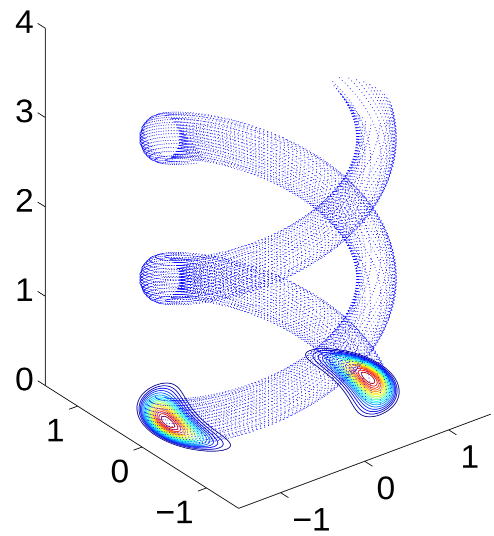

Note: The parameters are $r_0 = 1$, L = 0.5.

Measuring the angular velocity $\omega(t)$ obtained by DNS and comparing with the theoretical value obtained by the cutoff theory (Saffman, 1992) is one of the validation tests of the numerical code. The cutoff results are here semi-analytical since they use the quantities core size $a(t)$, distance $r_{max}(t)$ from the axis and core circulation $\Gamma(t)$ evolving in time and given by the DNS. The comparison is shown in Figure 4, and is found very satisfactory once the filaments have been destroyed and that the vortex has reached its quasi-steady state.

It should be noted that vorticity isocontours in Figure 3 are presented in a plane perpendicular to the z-axis: the curved/elongated shape adopted by the vortex for $t \geq 0.4$ corresponds in fact to a quasi-circular core shape when considered in an inclined plane perpendicular to the vortex tube.

This can also be seen on Figure 5, presenting a quasi-steady state made of two helical vortices. In this snapshot, the 3D helical structure of the vortex has been materialised. It is clearly seen that the cores are indeed close to circular while they are strongly deformed in the bottom plane perpendicular to z.

The numerical code thus makes it possible to obtain quasi-steady states of the Navier-Stokes equations with one or several helical vortices of given pitch. Note that the three-dimensional stability of these obtained solutions is not known since helical symmetry is enforced by the current formulation. Some states are stable, but other might be unstable with respect to perturbations breaking the helical symmetry. In this latter case however, the present numerical code is able to generate unstable basic helical flows that can be injected for instance in a fully three-dimensional code in order to determine various instability properties. This corresponds to future work.

5 Merging of two helical vortices

The above helical quasi-steady states evolve on a slow time scale associated to viscous diffusion. In the pure two-dimensional case ($L = \infty$), it is known that two identical vortices rotate around each other for a period of time proportional to Reynolds number (Josserand and Rossi, 2007). Eventually, their mutual distance suddenly decreases and, after some rapid oscillations, vanishes, indicating that the vortices have merged. The distance of one of the vortices from the z-axis during this process is plotted in Figure 6 (curve $L = \infty$). The merging time for this 2D case is 575.

Numerical simulations have been performed at the same Reynolds number Re_0 = 10,000 but for helical vortices at finite L values. Figure 6 shows that decreasing L progressively slows down the process; at $L = 3$ the merging time is 600, and can reach values as high as 1,400 at $L = 2$ (not shown). For the above values of L, the merging process is close to that occurring in the pure 2D case, as shown by the snapshots in Figure 7 (see two top rows).

When L is lowered to the value 1.3, another type of merging is observed: as shown in Figure 7 (third row), the vortices gently come into contact at t = 2,610: the helical vortex cores have grown through viscous diffusion up to a point where turns belonging to the two distinct vortices touch. Viscous diffusion then drives the system to a cylindrical annulus of vorticity (see t = 4,400). Thus, for L values close to 1.3, a very slow, merely diffusive merging process takes place, which involves successive vortex turns.

Figure 6 Merging of two helical vortices at Re_0 = 10,000 for different values of L

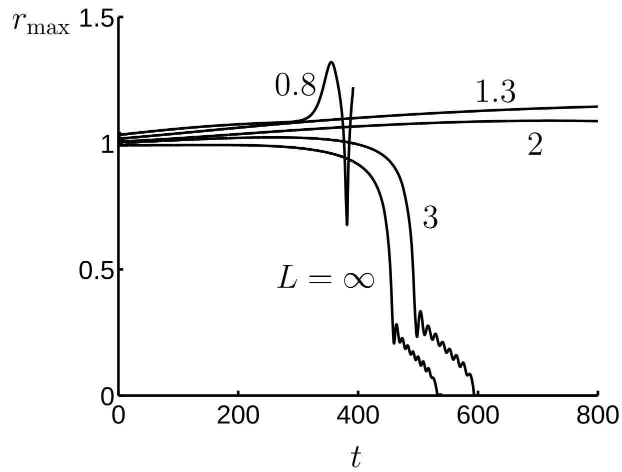

Notes: Time evolution of the distance r_{max} of one of the vortices from the axis. Initial helices $\Gamma_0 = 1$, $r_0 = 1$, $a_0 = 0.2$.

Figure 7 Snapshots of the helical vorticity component ω_B during the merging of two helical vortices with pitch L at Re_0 = 10,000 (see online version for colours)

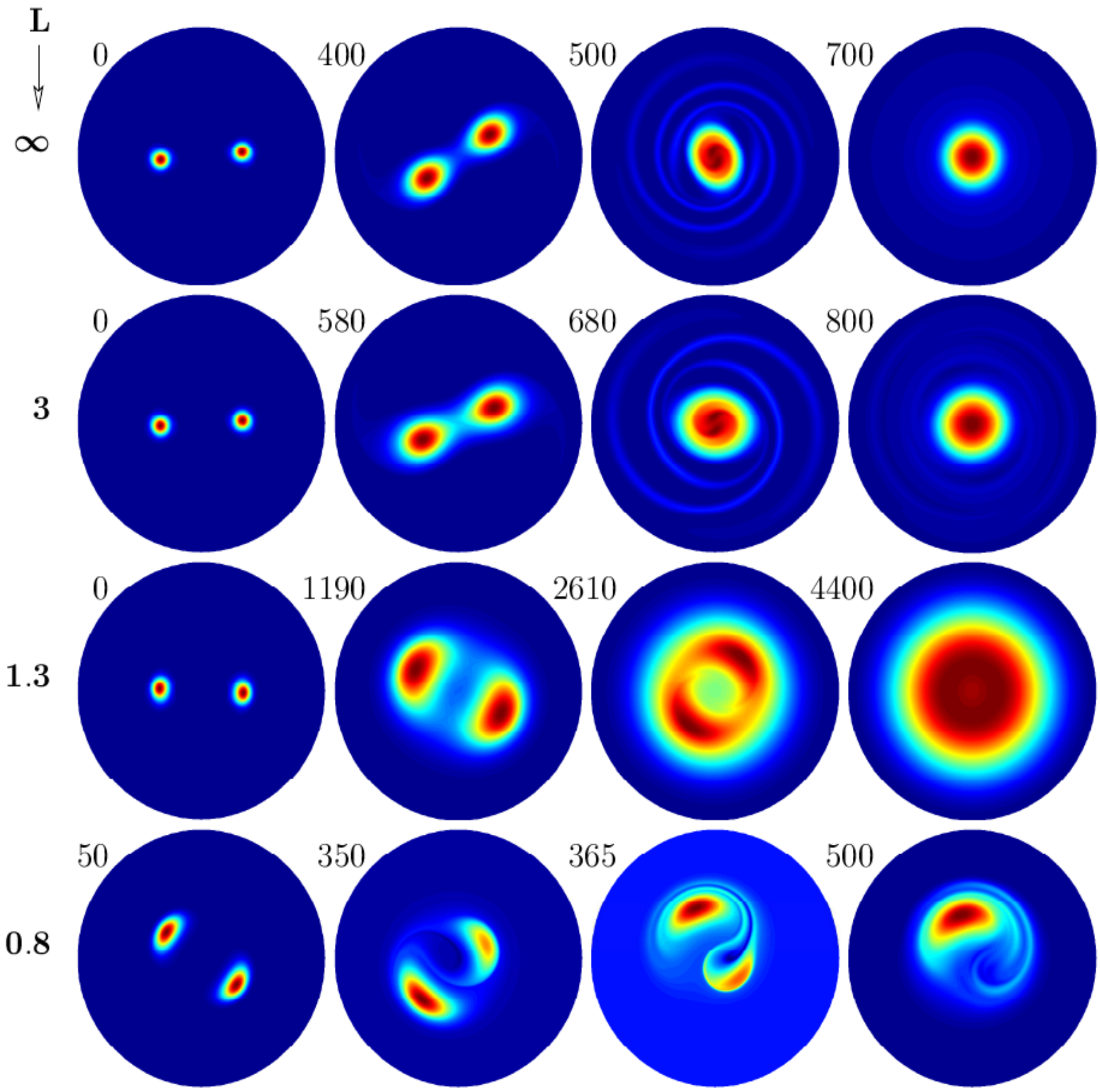

Note: Time evolution of the distance $r_{\max}$ of one of the vortices from the axis. Initial helices are such that $\Gamma_0 = 1$, $r_0 = 1$, $a_0 = 0.2$.

For smaller values of L, the dynamics is again much different. In Figure 6, the curve $r_{\max}(t)$ relative to $L = 0.8$ is seen to become strongly erratic at some time (here near $t = 300$). Beside the helical symmetry, the two-vortex initial condition is invariant through the transformation $\varphi \rightarrow \varphi + \pi$. For the largest investigated values of the reduced pitch ($L \geq 1.3$), this additional symmetry is preserved during the whole simulation. By contrast, the dynamics for $L = 0.8$ plotted in Figure 7 (bottom row) shows that it can break at some time (see $t = 350$), and the two helical vortices interact in a complex way. Symmetry breaking causes the periodicity along the direction ϕ to change from its initial value π to the value 2π, and therefore the periodicity along the axial direction z also changes from πL to $2\pi L$. The phenomenon has much in common with the subharmonic pairing instability of a row of straight vortices; here it involves two neighbouring turns and the patterns observed look similar to those obtained during the merging of two vortex rings (Riley and Stevens, 1992). Clearly the proximity of turns belonging to the two vortices at small L values is responsible for such interaction, and the structure resulting from their merging is a single helical vortex with large core size (see $t = 500$).

6 Conclusions

In this article, we present an original DNS code aimed at solving the Navier-Stokes equations for incompressible flow with helical symmetry. In this framework, the dynamics is governed by a set of three coupled equations for the helical components of vorticity ω_B, of velocity u_B and for the helical streamfunction ψ. The code is shown to give access to quasi-equilibrium states representing one or several helical vortices. The present code has several advantages: while taking into account three-dimensional effects of curvature and torsion, the resolution is basically of the 2D type, which allows for finer grids, higher Reynolds numbers and longer integration times. For example, this allows one to investigate the long-time dynamics of merging of two identical helical vortices at Re_0 = 10,000. It has been found that, at high values of the helix pitch (typically $L \geq 2$), the merging process is similar to the one obtained in pure 2D dynamics, but occurs on larger time scales as L is progressively decreased. At intermediate values of the pitch ($L \approx 1.3$), a slow diffusive-type of merging occurs between successive turns of the two-vortex system. At small values of the pitch (typically $L \leq 1$), adjacent turns interact as in a subharmonic instability process while remaining helically symmetrical. Of course, this latter symmetry may not hold in a three-dimensional framework, and some results of the present study should be confronted to fully 3D computations.

References

Daube, O. (1992) 'Resolution of the 2D Navier-Stokes equations in velocity/vorticity form by means of an influence matrix technique', *J. Comp. Phys.*, Vol. 103, No. 2, pp.402–414.

Delbende, I., Rossi, M. and Daube, O. (2011) 'DNS of flows with helical symmetry', Submitted to *Theor. Comput. Fluid Dynam.*

Fukumoto, Y. and Okulov, V.L. (2005) 'The velocity field induced by a helical vortex tube', *Phys. Fluids*, Vol. 17, No. 10, 107101.

Green, B.G., Gillies, E.A. and Brown, R.E. (2005) 'The flow field around a rotor in axial descent', *J. Fluid Mech.*, Vol. 534, pp.237–261.

Hardin, J.C. (1982) 'The velocity field induced by a helical vortex filament', *Phys. Fluids*, Vol. 25, No. 11, pp.1949–1952.

Josserand, C. and Rossi, M. (2007) 'The merging of two co-rotating vortices: a numerical study', *Eur. J. Mech. B/Fluid*, Vol. 26, No. 4, pp.779–794.

Kuibin, P.A. and Okulov, V.L. (1998) 'Self-induced motion and asymptotic expansion of the velocity field in the vicinity of a helical vortex filament', *Phys. Fluids*, Vol. 10, No. 3, pp.607–614.

Lucas, D. and Dritschel, D.G. (2009) 'A family of helically symmetric vortex equilibria', *J. Fluid Mech.*, Vol. 634, pp.245–268.

Moore, D.W. and Saffman, P.G. (1972) 'The motion of a vortex filament with axial flow', *Philos. Trans. R. Soc.*, London, Ser. A, Vol. 272, No. 1226, pp.403–429.

Riley, N. and Stevens, D.P. (1992) 'A note on leapfrogging vortex rings', *Fluid Dyn. Res.*, Vol. 11, No. 5, pp.235–244.

Saffman, P.G. (1992) *Vortex Dynamics*, Cambridge Monograph on Mechanics and Applied Mathematics, CUP.

Widnall, S.E. (1972) 'The stability of a helical vortex filament', *J. Fluid Mech.*, Vol. 54, pp.641–663.